Reactivity during bench-scale combustion of biomass fuels for carbon capture and storage applications

S. Pickard[a], S.S. Daood[b], M. Pourkashanian[c], W. Nimmo[c,*]

[a] *Low Carbon Technologies Doctoral Training Centre, University of Leeds, LS2 9JT, UK*
[b] *International Innovative Technologies Ltd., Gateshead, NE11 0BU, UK*
[c] *Energy Technology Innovation Institute, University of Leeds, LS2 9JT*

Abstract

Reactivities of four biomass samples were investigated in four combustion atmospheres using non-isothermal thermogravimetric analysis (TGA) under two heating rates. The chosen combustion atmospheres reflect carbon capture and storage (CCS) applications and include O_2 and CO_2-enrichment. Application of the Coats-Redfern method assessed changes in reactivity. Reactivity varied due to heating rate: the reactivity of char oxidation was lower at higher heating rates while devolatilisation reactions were less affected. In general, and particularly at the higher heating rate, increasing [O_2] increased combustion reactivity. A lesser effect was observed when substituting N_2 for CO_2 as the comburent; in unenriched conditions this tended to reduce char oxidation reactivity while in O_2-enriched conditions the reactivity marginally increased. Combustion in a typical, dry oxyfuel environment (30% O_2, 70% CO_2) was more reactive than in air in TGA experiments. These biomass results should interest researchers seeking to understand phenomena occurring in larger scale CCS-relevant experiments.

Keywords: biomass combustion, oxyfuel, oxygen-enrichment, Bio-CCS, TGA

*Corresponding author
Email address: w.nimmo@leeds.ac.uk (W. Nimmo)

1. Introduction

Combatting anthropogenic climate change and satisfying the forecast growth in global energy demand requires novel solutions for many established industries. Increasing pressure to limit and reduce greenhouse gas (GHG) emissions - particularly CO_2 - from power generation are widely understood to present a need to move away from unabated fossil fuel use. Reducing the emissions of CO_2 while maintaining a fleet of flexible thermal plant - required to balance and mitigate the variability of renewables generation against the inflexibility of nuclear generation - is seen as important by many nations. Two leading options to achieve this goal are to replace some or all of the fossil fuels with sustainably sourced carbonaceous fuels such as biomass or to capture and permanently store the CO_2 resulting from the combustion process. While neither biomass cofiring nor carbon capture and storage (CCS) are truly sustainable in the long-term (only dedicated biomass firing without CCS could be envisioned as such) they represent one of the strongest options developed nations possess to reduce their GHG emissions while largely maintaining the quality of life of their citizens in the coming decades. Indeed, "[w]ithout CCS, overall costs to halve CO_2 emission levels by 2050 increase by 70 %" [1]. Separately these processes could ideally offer substantial reductions in the emissions of CO_2 from electricity generation, but combined Bio-CCS projects could represent a net removal of CO_2 from the atmosphere. A net reduction of atmospheric CO_2 during Bio-CCS occurs as the CO_2 absorbed by plants during their photosynthetic growth stage is ultimately prevented from returning to the atmosphere being stored instead in deep geological formations. This is important since Bio-CCS is claimed to be "the only large-scale technology that can remove CO_2 from the atmosphere" [2] and with sustainably sourced fuels is able to produce power with lower GHG emissions than all other low-carbon generation technologies [3].

In the UK, early decarbonisation of the electricity system is seen as a priority in meeting the 2050 80% reduction targets since other sectors (e.g. transport and domestic heating) will require low-carbon electricity in order to reduce

their sector's carbon intensity [4]. Many technology roadmaps for the UK and globally strengthen the view that Bio-CCS is a necessary technology option for combatting climate change in the UK and around the world [1, 2, 5, 6].

1.1. Knowledge to Date

Conventional combustion of 100% biomass and cofiring with fossil fuels is widely practised on an industrial scale. However, CCS is still a developing technology which contains a wide range of configurational options and areas requiring further research [7]. A leading CCS technology option is oxyfuel combustion where, instead of selectively extracting CO_2 from a relatively dilute flue gas, the fuel is burnt in an environment that largely comprises of oxygen diluted by recycled flue gas (predominantly CO_2) which acts as a thermal diluent to match adiabatic flame temperatures to those seen in air-firing [8]. Through removing the largely inert nitrogen from the combustion process oxyfuel combustion is able to produce a flue gas far richer in CO_2 than conventional combustion processes requiring more conventional and economic gas clean up systems than envisioned for other CCS systems [9, 10].

As well as new power stations, the current fleet will continue to emit CO_2 unless mitigating options are taken. While some plant will be suitable for total retrofitting of technologies such as oxyfuel, in other situations alternative CCS options such as post-combustion capture (PCC) may be preferred. PCC typically uses a chemical or physical agent to selectively remove CO_2 from the flue gas. However, one drawback to this method is the magnitude of the cost and size of a CO_2-scrubbing plant that is necessarily large due to the relatively dilute CO_2 in conventional flue gas (typically $\sim 10\%$). One possibility for development in this area is to enrich the combustion air with oxygen, reducing the nitrogen content of the flue gas and hence concentrating CO_2 which could reduce the size and cost of PCC components, albeit at the extra cost of supplying oxygen. However, in addition to the potential logistical benefits, this technology option has been demonstrated to enhance combustion efficiency while simultaneously reduce nitrous oxide emissions when oxidant staging with over-fired air is used

[11, 12].

1.2. Experimental Background

While bench-scale combustion techniques differ from full-scale plant in a number of ways, thermogravimetric analysis is a useful analogue for full-scale combustion that has been widely adopted to assess trends in fuel reactivity in both air and oxyfuel combustion scenarios, for example [13–15]. As standalone technologies biomass combustion and CCS have received much attention. However, a knowledge gap exists where little technical data has been published that concentrates on biomass combustion in situations applicable to CCS. In this work the behaviour of four biomass fuels in four combustion atmospheres which are useful to the the development of CCS technologies are investigated to provide preliminary indications of their behaviour in novel combinations of fuel and combustion atmospheres. This work forms a part of a suite in which the fuels and combustion environments investigated at bench-scale are then used to inform the results of similar combustion tests carried out at pilot-scale [16].

Addressing climate change is a global challenge and the fuels tested in this study, while typical in the UK energy mix, are common outside of the UK so it is hoped the findings will be of wider interest.

2. Materials and Methods

Three biomass resources - short rotation coppiced willow (SRC), miscanthus (MC) and reed canary grass (RCG) - were grown in the North of England by the BioReGen project [17]. Shea Meal (SM) supplied by RWE NPower was also included to compare with previous work [18]. Proximate analysis of the fuels was carried out by TGA analysis of mass loss in a nitrogen atmosphere with a temperature ramp rate of $20\,\mathrm{K\,min^{-1}}$. Analysis of the lignocellulosic contents of biomass was conducted by several wet chemistry stages, as detailed in [19]. Results of analysis of the fuels are shown in table 1. The negative value for lignin derived using the acid detergent lignin (ADL) method arises as the

ADL measured value is less than the ash content of the fuel which suggests some of the ash components are solubilised by acid solutions. While this is less apparent for the samples containing lower amounts of ash, the negative value for RCG is thought to be due to the relatively high ash content (8.1%) acid solubility of particularly Ca and Na [20]. While the Klason and ADL methods for measuring lignin appear similar, differences of the magnitude observed in table 1 are common, see for example [19].

2.1. Sample Preparation

All of the UK-grown biomasses were harvested, dried and milled to pass through a sieve of 0.5 mm. In an attempt to separate experimental physical characteristics from those of a chemical nature and to ensure homogeneity in small sample sizes, it was necessary to further reduce the size of the particles. Mass transfer effects during thermal treatment have been shown to be largely mitigated once particle size is reduced to approximately 200 µm [21]. To avoid the escape of volatile species and/ or waxy deposits, the biomass samples were milled using a SPEX 6770 Freezer Mill which uses liquid nitrogen to ensure samples remain solid during milling [22, 23]. All samples were milled until they passed easily through a 212 µm sieve.

2.2. Experimental Procedure

The data analysed in this work was first generated according collection methods similar to those detailed in ASTM standards E1641 and E2550. For each experiment 5 ± 0.5 mg of each biomass sample was accurately measured into an open alumina crucible and the sample was introduced to a Mettler-Toledo TGA/DSC1 device. In this equipment, the thermobalance is coupled to a differential scanning calorimeter. While not used in analysing reactivity, the latter function was used alongside the TGA data to highlight the various reaction stages that occur during combustion. Once air was purged by the test atmosphere the sample was then heated to 383 K and held for a 30 min period to drive off moisture. The sample was then heated at the test heating rate (β) to a

temperature of 1023 K while the test atmosphere was fed into the chamber at a rate of 50 ml min^{-1}. The sample was held at the final temperature for a further 30 min period to ensure combustion was complete.

The combustion of each biomass sample was studied in four oxidising atmospheres. Air (21% O_2, 79 % N_2) was the reference case. Consistent with similar work in this field [14], the composition of the oxyfuel atmosphere was chosen to be similar to that reported in the literature and consists of an enriched O_2 level compared to air and thus was labelled En-Oxy (30 % O_2, 70 % CO_2). In order to investigate the effect of increasing oxygen concentration and substituting N_2 for CO_2 separately, an oxygen-enriched air (En-Air: 30 % O_2, 70 % N_2) and an unenriched oxyfuel condition (Oxy: 21 % O_2, 79 % CO_2) were also included in the experimental design. Although the Coats-Redfern method only requires a single heating rate to generate reactivity parameters [24], each of the TGA tests was repeated at heating rates of 10 and 40 K min^{-1} to increase the robustness of the results.

2.3. Analysis of Experimental Data

Previous work presents a detailed methodology which reports that an extension of the Coats-Redfern technique may be used to compare reactivities for complex decompositions in a robust, reliable fashion suitable for fuel screening [16]. Thus, the procedure for identifying reactions, selecting a data range for curve fitting and estimation of rate parameters outlined therein was followed in the current work. An outline of this methodology is presented below.

First, a formalised procedure in which the derivative thermogram (DTG) graph is analysed graphically was used to identify constituent reactions and select a data range for curve fitting. From the analysis of the DTG of each of the samples, the decomposition of each of the biomasses was assumed to occur due to three independent, parallel, first-order pseudo-reactions. No smoothing of the TGA data was employed during the analysis procedure. The standard Coats-Redfern procedure for first-order reactions was then used to estimate the reactivity parameters - apparent activation energy (E_A) and pre-exponential

constant (A) - for each of these reactions separately. This involves plotting $-\ln\left(\ln\left(1-\alpha\right)/T^2\right)$ against $1/T$ where α represents the extent of reaction at a given temperature (T) and is defined by the mass (m) at initial (i) and final (f) points as $\alpha = \left(m_i - m_T\right)/\left(m_i - m_f\right)$. The slope of the line of best fit to the data is equal to $-E_A/R$ and the intercept with the y-axis equals $\ln\left(AR/\beta E_A\right)$ where R is the universal gas constant and β is the heating rate.

To understand how well these parameters characterise the overall decomposition profiles the estimated values are then substituted into an Arrhenius-based reaction model reflecting the assumption of three independent, first-order, parallel reactions. Iterating this model across the TGA temperature range attempted to recreate the decomposition profile of the TGA curve. The correlation between the recreated profile and its derivative and the original mass and DTG profiles is then quantified by the square of the Pearson Correllation Coefficient (r^2).

The compensation effect between kinetic parameters is widely documented in the literature, for example see [24–26]. In this work the purpose is to analyse trend changes between combustion atmospheres rather than provide numerical values for kinetic parameters, as has been shown to be possible in previous work[16]. Thus, in an attempt to mitigate the compensation effect, trends in reactivity between different combustion scenarios comparisons are assessed by normalising the reactivity of a given scenario to a reference case value for apparent activation energy ($E_{A,0}$) and pre-exponential function (A_0) using eq. (1). For traceability of results the estimated parameters are provided in supplementary material.

$$S_i = 1 - \frac{\frac{E_{A,i}}{E_{A,0}}}{\frac{\ln A_i}{\ln A_0}} \tag{1}$$

where if

- $S_i < 0$ then the decomposition is less reactive than the reference case
- $S_i = 0$ then the decomposition and the reference case are equally reactive
- $S_i > 0$ then the decomposition is more reactive than the reference case

3. Results and Discussion

The four biomass resources were processed in the TGA device for the four combustion atmospheres at two heating rates. The changes in mass and DTG against temperature for each of these experiments are shown in Figures 1 and 2 for $\beta = 10$ and 40 $\mathrm{K\,min^{-1}}$ respectively. The temperature ranges of each of the reactions was found to change between experiments; Figure 3 illustrates the effect of heating rate and combustion atmosphere on these ranges. The temperatures quoted in the following discussion relate to the identified temperature ranges found by following the procedure and not directly to changes observed on the DTG.

The three energy crops - SRC, RCG and MC - display similar decomposition DTG profiles and temperature ranges for the three reactions. Considered alongside the similarities in proximate and ultimate analyses shown in table 1, this may indicate the substructures of each of these samples may also be comparable. In air these decompositions can be broadly described by the onset of an initial endothermic reaction at approximately 490 K for $\beta = 10\,\mathrm{K\,min^{-1}}$ and $\approx 515\,\mathrm{K\,min^{-1}}$ for $\beta = 40\,\mathrm{K\,min^{-1}}$. Comparison of the temperature range of this reaction with literature suggests this reaction may be due to the release of volatiles during the breakdown of hemi-cellulose materials [27–29]. The decline of this initial reaction then overlaps slightly with an increase of the rate of an exothermic reaction forming a shoulder in the DTG curve in the region of 575 and 595 K for the energy crops decomposing at the respective heating rates in air which may be due to the oxidation of volatiles released due to the decomposition of cellulose materials. At temperatures of approximately 650 and 675 K the final reaction - which is also exothermic - is found to take control of the decomposition continuing until $\approx$ 765 and 820 K. Reactions in this temperature range are often attributed to the oxidation of char and from comparison with the proximate analysis here it is assumed to be due to the more stable lignin-derived volatlile components [28].

Dissimilar to the grasses and willow, SM tends to begin devolatilisation at a

lower temperature (approximately 35 K and 50 K) than the other biomasses and the transition between the endothermic and exothermic devolatilisation stages also occurs at significantly lower temperature (535 K for $\beta = 10\,\mathrm{K\,min^{-1}}$ and 555 K for $\beta = 40\,\mathrm{K\,min^{-1}}$). A lower temperature devolatilisation may be due to weaker macromolecular bonds [14], which may also be relevant here.

The DTG profile for the decomposition of SM has less defined reaction peaks and, particularly in the temperature interval of 650 K to 750 K, a complex series of reactions that convolute the DTG seem to be occurring. Assuming the complex decomposition for SM can be represented by 3 pseudo-reactions has the effect of increasing the temperature range of the second and third reactions in SM's decomposition causing the reactions identified for the decomposition of SM to span the widest temperature range.

The fastest mass-loss for each of the energy crops occurs during the second pseudo-reaction in all oxidising atmospheres at temperatures ranging from 590 K to 610 K and 615 K to 640 K for $\beta = 10$ and $40\,\mathrm{K\,min^{-1}}$ respectively. The SM DTG profile shows far more gradual changes in rate of mass-loss and as a result the peak reaction rate is lower than the other samples with a mass-loss sustained across a wider temperature range. Indeed, when SM was heated at the slower heating rate the peak reaction rate is found for the char oxidation stage rather than the volatile combustion reaction which displays the fastest mass-loss in the other samples. This may be explained as the SM displays a higher char:volatiles ratio than the grasses and willow and a significantly higher ratio of lignin to holocellulose with lignin generally understood to decompose across a wider temperature range.

3.1. Reaction Temperature Ranges

3.1.1. Effect of Heating Rate

For the three energy crops every reaction was retarded and elongated when the heating rate (β) was increased from $10\,\mathrm{K\,min^{-1}}$ to $40\,\mathrm{K\,min^{-1}}$. For the energy crops the averaged temperatures for the start of reaction one increased from 495 K to 512 K and the temperature at which crossover between the first

two reactions occurred increased from 572 K to 591 K. The span of temperatures for the final, char oxidation reaction increased from an average of 649 K to 765 K for $\beta = 10\,\mathrm{K\,min^{-1}}$ to 676 K to 818 K when $\beta = 40\,\mathrm{K\,min^{-1}}$. The larger fixed carbon content of SM caused the final reaction in the overall decomposition to be extended by approximately 50 K further than for the energy crops. The elongation of the final the reaction temperature range for each of the samples suggests this reaction may not be kinetically controlled by the bulk system temperature and instead dependent on other experimental factors that contribute to mass and heat transfer within the particles. This is despite the particle sizes being reduced to $< 212\,\mu\mathrm{m}$.

3.1.2. Effect of Reaction Atmosphere

Figure 3 suggests that changes to the combustion atmosphere have a negligible effect on the endothermic devolatilisation of the biomass samples (R1). However, in atmospheres with an enriched level of oxygen reactions two and three tended to span a reduced, narrower temperature range for a given heating rate than their unenriched counterparts, suggesting increased $[O_2]$ allows both more intense combustion of volatiles and oxidation of chars. This is in broad agreement with the literature - see [15] for example - though whether the volatile combustion or char oxidation is more affected was observed to vary between experiments. This does however suggest that in these experiments the rate of delivery of oxygen to the particle surface affects the rate of release of the volatile components as well as affecting char oxidation.

Substituting the base gas of N_2 with CO_2 seems to have a complex but considerably smaller effect on the temperature range across which the reactions occur than increasing $[O_2]$. The temperature range for the RCG reactions appears to show almost no effect of changing from N_2-based to CO_2-based atmospheres while the SM results suggest a slight elongation of the reaction temperature range in CO_2-based environments. In unenriched conditions substituting N_2 with CO_2 either had no effect or elongated slightly the total temperature range, similar to that reported elsewhere [15, 30]. However, in O_2-enriched atmo-

spheres no clear trends can be extracted from the results, perhaps suggesting uncertainty in identification of reactions reduces the accuracy of this technique in robustly investigating subtle differences, requiring instead further analysis of the data, such as that below.

3.2. Relative Reactivity (S_i)

The apparent activation energy (E_a) and pre-exponential factor (A) for each of the reactions in each decomposition and how well the estimated parameters characterise the total decomposition (r^2) were calculated according to the procedure detailed in [16]. For traceability of data these results are tabulated in the supporting material. However, noting the compensation effect it is felt undesirable to discuss the changes in kinetic parameters separately and instead this work will only discuss the changes in total reactivity (incorporating both the apparent activation energy and pre-exponential factor). It has already been remarked that little similar work exists in the literature and comparisons with that which does is somewhat problematic. For example the work in [15] compares characteristic temperatures between air and oxyfuel only but does not estimate reactivity parameters, the work in [30] compares air and oxyfuel combustion of coal chars by estimating the apparent activation energy of the char reaction using multiple heating rates but only at at 10 % [O_2]. Additionally, while the work in [14] evaluates biomasses decomposing in the same atmospheres the work did not estimate reactivity parameters from the TGA analysis. Nevertheless, where possible literature comparable with the findings are discussed below.

3.2.1. Effect of Heating Rate

One assumption regularly employed during the extraction of kinetic parameters from non-isothermal TGA work is that the parameters are independent of the experimental heating rate so long as the magnitude of variation is small. To investigate this a comparison between the results at different heating rates is investigated in fig. 4 where $\beta = 10\,\mathrm{K\,min^{-1}}$ is used as the reference case for the higher heating rate. This figure shows that the reactivities predicted for the

grasses - RCG and MC - at the higher heating rate are typically within 5 % of those estimated at the lower heating rate. However, the results for SRC and SM suggest in all cases the final reaction is substantially less reactive at the higher heating rate. Taking all the results together this supports the claim that no consensus has emerged whether increases in heating rate reduces the kinetic rate of reactions [24]. Moreover, it is considered beyond the scope of this work to investigate the effect of heating rate on reactivity parameters or the methods of estimating them, instead focusing on the trend changes due to changing combustion atmospheres. Thus, rather than increasing the uncertainty by averaging the results for S_i the relative reactivities are calculated and presented for each heating rate individually. Figures 5a and 5b show the results for 10 and 40 $\mathrm{K\,min^{-1}}$ heating rates, respectively, and the results are discussed by fuel before more general conclusions are drawn concerning the effects of changing the combustion atmospheres.

3.2.2. SRC

The SRC samples are observed to behave in a similar fashion under both heating rates. In atmospheres with enriched $[O_2]$ the final char reaction was observed to be more reactive than the corresponding unenriched scenarios. In the oxyfuel (CO_2-based) atmospheres enriching the $[O_2]$ also caused an increase in the reactivity of the second reaction though this was less readily observed in N_2-based environments. No trend can be elucidated concerning how reactivity changes for the first reaction depending on the combustion environment, though most changes observed are small corroborating the findings shown in fig. 3. At the slower heating rate for unenriched atmospheres replacing N_2 with CO_2 tended to have a small effect on each of the reactivities while at the faster heating rate a substantial reduction in reactivity of the char oxidation was witnessed, perhaps suggesting slower diffusion of O_2 in CO_2 is to some extent limiting the reaction. However, the fact that this reduction was not seen at higher $[O_2]$, where small increases in S_i were observed, may suggest the enrichment of O_2 sufficiently counters the reduction in its mobility. The second reaction stage is

responsible for approximately 50% of the total mass loss and in all atmospheres this was observed to be more reactive than combustion in air. Substitution of N_2 with CO_2 tended to slightly increase S_i for this reaction in all conditions tested.

3.2.3. MC

At the slower heating rate increasing $[O_2]$ was observed to very slightly increase the reactivities of reactions 2 and 3, though at $40\,\mathrm{K\,min^{-1}}$ these oxidative reactions greatly benefitted from the increased oxygen concentration particularly the char-oxidation. At unenriched conditions substituting N_2 with CO_2 for an oxyfuel environment caused the reactivity of the char-oxidation to fall at both heating rates. Although more pronounced at the higher heating rate, an increase in reactivity of reactions 2 and 3 when switching to oxyfuel is also seen at enriched conditions for both heating rates.

At the slower heating rate increasing $[O_2]$ was observed to slightly increase the reactivities of reactions 2 and 3. However, at $40\,\mathrm{K\,min^{-1}}$ these oxidative reactions greatly benefitted from the increased oxygen concentration. The second reaction was again the most important in terms of total mass representing approximately 45% of the total mass loss during the decomposition. In O_2-enriched conditions the apparent reactivity for this reaction increased. Particularly under faster heating rates, the reactivity of the final reaction was also increased with increasing $[O_2]$. In the char oxidation stage substituting N_2 with CO_2 reduced reactivity in unenriched conditions but slightly increased the value of S_i when $[O_2]$ was enriched.

3.2.4. RCG

RCG shows the same trend as MC above in the second reaction, which is responsible for a similar amount of the total mass loss, with the value of S_i increasing in O_2-enriched conditions at lower heating rates and in the char oxidation stage at the higher heating rate. Comparison with the DTGs suggest the reason for this shift in increased S_i from R2 to R3 may be due to changes in

the way the DTG is analysed rather than changes in S_i between the reactions. At low heating rates substituting N_2 with CO_2 was observed to have a relatively minor effect on the reactivities. However, at $40\,K\,min^{-1}$ reactions 2 and 3 were observed to increase in reactivity when switching to an oxyfuel environment of comparable $[O_2]$.

3.2.5. SM

The relatively poor correlation between the reconstructed mass and DTG curves for the SM samples indicate the method can less robustly analyse the changes in relative reactivity for this sample and emphasise the need for care when attempting to interpret the results. Comparing S_i with the DTGs in Figures 1 and 2 it can be observed that when increasing the oxygen concentration compared to the unenriched state the reactivity of the final reaction increases while the same reaction was reduced when the atmosphere was changed to be CO_2-based.

3.3. Overall Results

Although the results for the different fuels show some variation, some overall conclusions may be drawn. The energy crops behaved in a similar fashion while changes to the reactivity of SM were unique to that fuel. Overall, S_i, reaction temperature ranges and DTG results show that enriching the concentration of oxygen in the combustion atmosphere is the most important factor affecting reactivity and increases the reactivity of combustion occurring during either one or both of reactions 2 or 3. This is in agreement with reported findings for coal chars [30], though with only two oxygen concentrations here it is not possible to predict dependence of the reaction on the O_2-concentration as is carried out in that work. The impact on reactivity was found to be greater at the higher heating rate where it is suggested $[O_2]$ has a stronger rate-limiting effect due to the diffusion of O_2 to the char surface required for char oxidation.

Similar to the findings in the literature, no clear trends were observed when substituting N_2 with CO_2, which appeared to be dependent on the experimental

set up. At a heating rate of $10\,\mathrm{K\,min^{-1}}$ in unenriched conditions replacing air with a CO_2-based atmosphere tends to reduce the reactivity relative to air of the final char-oxidation reaction. However, this trend was not observed for all fuels at the fastest heating rate. Conversely, in O_2-enriched conditions the oxyfuel environment appeared to be marginally more reactive than that with N_2 as the base gas. This result is unlikely to be observed in practical combustion because the operation of the TGA instrument involves ensuring a given temperature within the combustion chamber. Therefore, as noted in [30], unlike in a furnace where the higher heat capacity of CO_2 would reduce gas and particle temperatures (hence depressing apparent reactivity), the temperature depression is not witnessed in the TGA instrument, thus this depression of reactivity is not seen. As for the slight increase in reactivity, although the CO_2-gasification reaction does not significantly affect decomposition until higher temperatures this could also contribute a small amount to an increased reactivity. Additionally, the increased heat capacity of CO_2 could lead to marginally higher particle temperatures as more energy is contained in the system at any given temperature.

Comparing a typical dry oxyfuel combustion atmosphere of 30 % O_2 with combustion in air finds that the latter is more reactive during both the combustion of volatiles and char oxidation stages. However, the extent to which this phenomenon exists at large-scale combustion with much more rapid heating rates is unclear. On the one hand the increased heat capacity of CO_2 is likely to reduce the gas and particle temperatures compared to a N_2-based environment. However, in practice, oxyfuel combustion will likely be carried out in oxygen-enriched conditions that elevate the furnace temperatures by reducing the thermal diluent and intensifying the combustion process promoting higher reaction rates.

4. Conclusions

Four biomass samples decomposing in CCS-relevant atmospheres were analysed by TGA at two heating rates. Application of the Coats-Redfern method

assessed changes in reactivity between tests. Char oxidation was less reactive at higher heating rates while the devolatilisation reactions were less affected. In general, and particularly at the higher heating rate, increasing [O_2] increased combustion reactivity. A lesser effect was observed when substituting N_2 with CO_2 as the comburent; char oxidation reactivity tended to fall in unenriched conditions while in O_2-enriched conditions reactivity marginally increased. These results should interest researchers seeking to understand phenomena occurring in larger scale Bio-CCS-relevant experiments.

5. Acknowledgements

This work was funded by EPSRC through the Low Carbon Technologies Doctoral Training Centre and through Seedcorn funding from the University of Teesside. The authors are grateful to Dr. R. Lord and RWE for supplying the biomass samples used in this work and Dr S. Lister for carrying out the lignocellulosic analysis. In addition, the laboratory support and advice provided by Dr. A.M. Cunliffe and Mr. S. Micklethwaite and guidance from Dr. L.I. Darvell during sample preparation is gratefully acknowledged.

6. References

[1] IEA. Technology Roadmap: Carbon Capture and Storage. Technical report, International Energy Agency (IEA), 2009.

[2] ZEP. Biomass with CO2 Capture and Storage (Bio-CCS) The way forward for Europe. Technical report, European Technology Platform for Zero Emission Fossil Fuel Power Plants, 2012.

[3] O Lucon, A Rahman, J Christensen, F Denton, J Fujino, G Heath, S Kadner, M Mirza, A Schlaepfer, A Shmakin, Climate Change, Y Sokona, K Seyboth, P Matschoss, P Eickemeier, and G Hansen. Renewable Energy in the Context of Sustainable Development. In C. von Stechow O. Edenhofer, R. Pichs-Madruga, Y. Sokona, K. Seyboth, P. Matschoss, S. Kadner, T.

Zwickel, P. Eickemeier, G. Hansen, S. Schlömer, editor, *IPCC Special Report on Renewable Energy Sources and Climate Change Mitigation*, chapter Chapter 9, pages 707–790. Cambridge University Press, Cambridge, UK, 2011.

[4] DECC. 2050 Pathways Analysis. Technical Report July, UK Department of Energy and Climate Change, London, 2010.

[5] DECC. CCS Roadmap. Technical Report April, Department of Energy and Climate Change, London, 2012.

[6] DECC, DEFRA, and DfT. UK Bioenergy Strategy. Technical Report April, Department of Energy and Climate Change, Department for the Environment, Food and Rural Affairs, Department for Transport, London, 2012.

[7] APGTF. Cleaner Fossil Power Generation in the 21 st Century Maintaining a Leading Role. Technical Report August, Advanced Power Generation Technology Forum, 2011.

[8] IPCC. Carbon Dioxide Capture and Storage. Technical Report 13, Intergovernmental Panel on Climate Change, July 2005.

[9] J.P. P Smart and G.S. S Riley. Use of oxygen enriched air combustion to enhance combined effectiveness of oxyfuel combustion and post-combustion flue gas cleanup Part 1 - combustion. *Journal of the Energy Institute*, 85(3):123–130, August 2012.

[10] K Zanganeh and a Shafeen. A novel process integration, optimization and design approach for large-scale implementation of oxy-fired coal power plants with CO2 capture. *International Journal of Greenhouse Gas Control*, 1(1):47–54, April 2007.

[11] W. Nimmo, S.S. S Daood, and B.M. M Gibbs. The effect of O2 enrichment on NOx formation in biomass co-fired pulverised coal combustion. *Fuel*, 89(10):2945–2952, October 2010.

[12] S.S. Daood, W. Nimmo, P. Edge, and B.M. Gibbs. Deep-staged, oxygen enriched combustion of coal. *Fuel*, (101):2–11, February 2011.

[13] Paolo Davini, Paolo Ghetti, and De Michele. Investigation of the combustion of particles of coal. *Fuel*, 75(9):1083–1088, 1996.

[14] Nur Sena Yuzbasi and Nevin Selçuk. Air and oxy-fuel combustion characteristics of biomass/lignite blends in TGA-FTIR. *Fuel Processing Technology*, 92(5):1101–1108, May 2011.

[15] M. V. Gil, J. Riaza, L. Álvarez, C. Pevida, J. J. Pis, and F. Rubiera. A study of oxy-coal combustion with steam addition and biomass blending by thermogravimetric analysis. *Journal of Thermal Analysis and Calorimetry*, 109(1):49–55, February 2012.

[16] S. Pickard, S. S. Daood, M. Pourkashanian, and W. Nimmo. Robust Extension of the CoatsRedfern Technique: Reviewing Rapid and Realiable Reactivity Analysis of Complex Fuels Decomposing in Inert and Oxidizing Thermogravimetric Analysis Atmospheres. *Energy & Fuels*, 27(5):2818–2826, May 2013.

[17] Richard Lord, Janet Atkinson, Andy Lane, Jonathan Scurlock, and Graham Street. BIOMASS, REMEDIATION, RE-GENERATION (BioReGen LIFE PROJECT): RE-USING BROWNFIELD SITES FOR RENEWABLE ENERGY CROPS. In *ConSoil*, pages 3–6, Milan, 2008.

[18] S Munir, S S Daood, W Nimmo, a M Cunliffe, and B M Gibbs. Thermal analysis and devolatilization kinetics of cotton stalk, sugar cane bagasse and shea meal under nitrogen and air atmospheres. *Bioresource technology*, 100(3):1413–8, February 2009.

[19] Marion Carrier, Anne Loppinet-Serani, Dominique Denux, Jean-Michel Lasnier, Frédérique Ham-Pichavant, François Cansell, and Cyril Aymonier. Thermogravimetric analysis as a new method to determine the lignocel-

lulosic composition of biomass. *Biomass and Bioenergy*, 35(1):298–307, January 2011.

[20] Ann G Kim, George Kazonich, and Michael Dahlberg. Relative solubility of cations in Class F fly ash. *Environmental science & technology*, 37(19):4507–11, October 2003.

[21] Hong Lu, Elvin Ip, Justin Scott, Paul Foster, Mark Vickers, and Larry L. Baxter. Effects of particle shape and size on devolatilization of biomass particle. *Fuel*, 89(5):1156–1168, May 2010.

[22] J M M Adams, A B Ross, K Anastasakis, E M Hodgson, J A Gallagher, J M Jones, and I S Donnison. Seasonal variation in the chemical composition of the bioenergy feedstock Laminaria digitata for thermochemical conversion. *Bioresource technology*, 102(1):226–34, January 2011.

[23] J.M. Jones, T.G. Bridgeman, L.I. Darvell, B. Gudka, A. Saddawi, and A. Williams. Combustion properties of torrefied willow compared with bituminous coals. *Fuel Processing Technology*, 101:1–9, September 2012.

[24] John E. White, W. James Catallo, and Benjamin L. Legendre. Biomass pyrolysis kinetics: A comparative critical review with relevant agricultural residue case studies. *Journal of Analytical and Applied Pyrolysis*, 91(1):1–33, May 2011.

[25] W De Jong, G Dinola, B Venneker, H Spliethoff, and M Wojtowicz. TG-FTIR pyrolysis of coal and secondary biomass fuels: Determination of pyrolysis kinetic parameters for main species and NOx precursors. *Fuel*, 86(15):2367–2376, October 2007.

[26] Sergey Vyazovkin, Alan K. Burnham, José M. Criado, Luis a. Pérez-Maqueda, Crisan Popescu, and Nicolas Sbirrazzuoli. ICTAC Kinetics Committee recommendations for performing kinetic computations on thermal analysis data. *Thermochimica Acta*, 520(1-2):1–19, June 2011.

[27] Haiping Yang, Rong Yan, Hanping Chen, Dong Ho Lee, and Chuguang Zheng. Characteristics of hemicellulose, cellulose and lignin pyrolysis. *Fuel*, 86(12-13):1781–1788, August 2007.

[28] Colomba Di Blasi. Modeling chemical and physical processes of wood and biomass pyrolysis. *Progress in Energy and Combustion Science*, 34(1):47–90, February 2008.

[29] A Borrego, L Garavaglia, and W Kalkreuth. Characteristics of high heating rate biomass chars prepared under N2 and CO2 atmospheres. *International Journal of Coal Geology*, 77(3-4):409–415, January 2009.

[30] Hao Liu. Combustion of Coal Chars in O 2 /CO 2 and O 2 /N 2 Mixtures: A Comparative Study with Non-isothermal Thermogravimetric Analyzer (TGA) Tests. *Energy & Fuels*, 23(9):4278–4285, September 2009.

Table 1: Combined results of fuel characterisation studies

Fuel	SRC	MC	RCG	SM
Proximate analysis (%), ar:				
Moisture	6.0	5.5	5.8	7.5
Volatile matter (VM)	72.4	74	68.5	53.8
Fixed carbon (FC)	18.7	17.3	17.6	31.9
Ash	2.9	3.3	8.1	6.9
Ultimate analysis (%), ar:				
C	47.7	46.4	42.2	48.6 [a]
H	6.0	5.8	5.4	5.9 [a]
N	0.4	0.3	1.4	2.9 [a]
S	0.0	0.0	0.0	0.2 [a]
O[b]	43.0	44.3	42.8	37.5 [a]
C:H	8.0	8.0	7.8	8.3 [a]
C:O	1.1	1.0	1.0	1.3 [a]
Lignocellulosic content(%), ar:				
Hemicellulose	11.7	22.4	27.5	10.9
Cellulose	48.0	47.6	31.2	2.9
Lignin (ADL)	14.0	6.0	-2.0	24.4
Lignin (Klason)	27.2	23.0	20.0	41.6

[a] Shea meal data from [11]; [b] By difference;

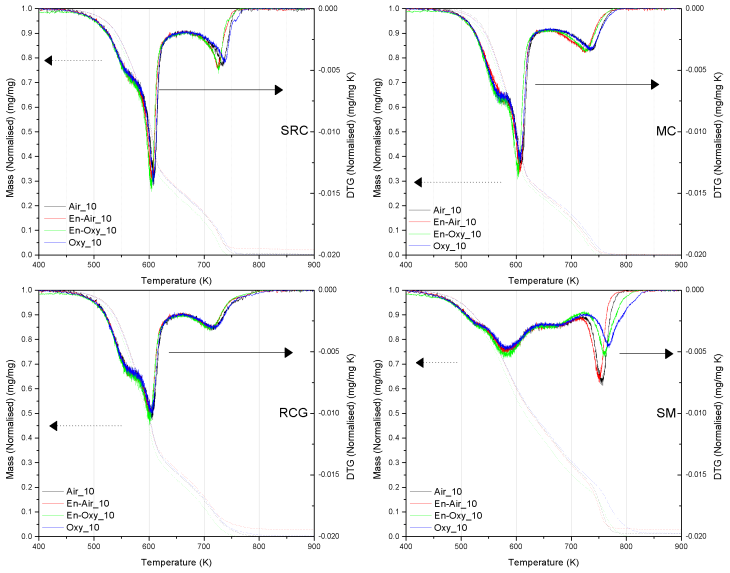

Figure 1: Mass and DTG results for short rotation coppiced (SRC) willow, miscanthus (MC), reed canary grass (RCG) and shea meal (SM) decomposing in different combustion atmospheres at a heating rate of $10\,\mathrm{K\,min^{-1}}$

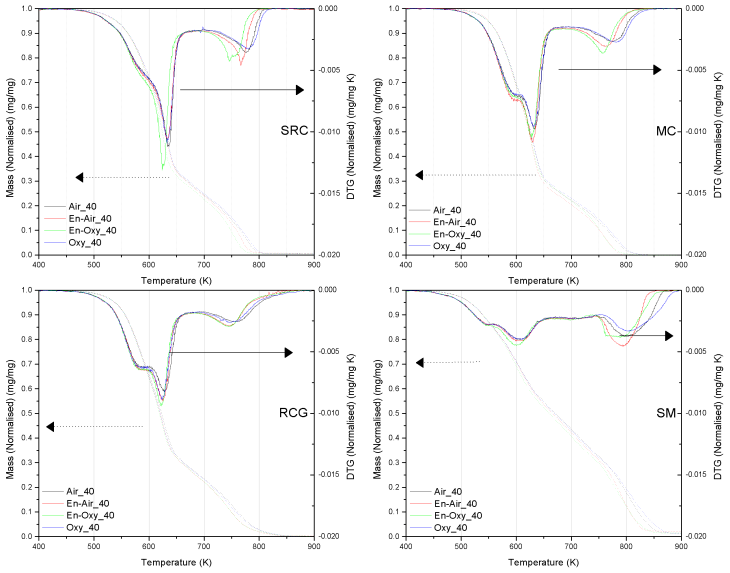

Figure 2: Mass and DTG results for short rotation coppiced (SRC) willow, miscanthus (MC), reed canary grass (RCG) and shea meal (SM) decomposing in different combustion atmospheres at a heating rate of $40\,\mathrm{K\,min^{-1}}$

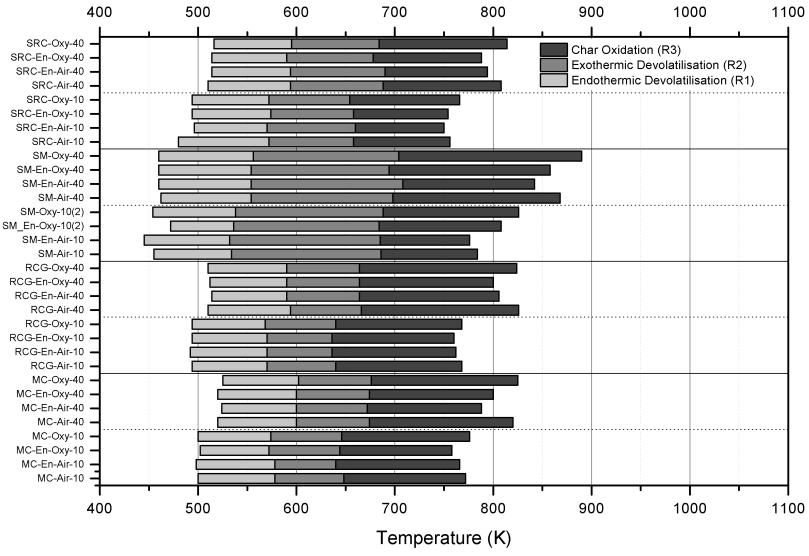

Figure 3: Variation in identified reaction zones for each of the biomass samples decomposing in different combustion atmospheres under 10 and 40 K min^{-1}

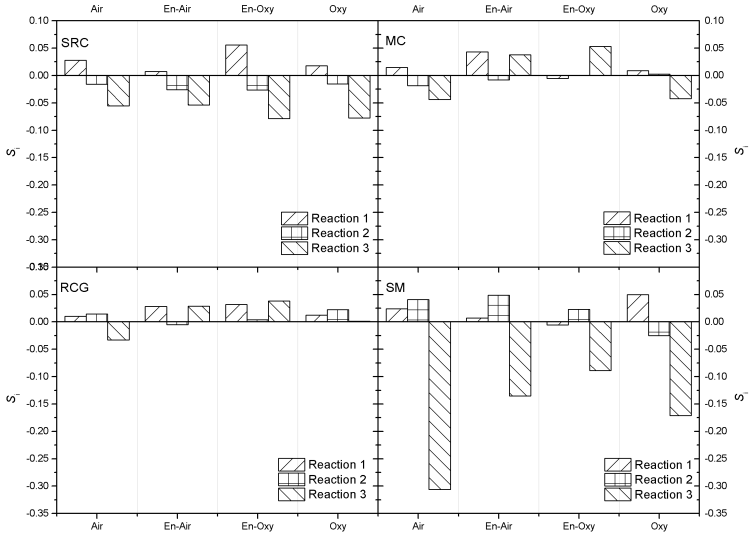

Figure 4: S_i comparison between estimated reactivity of sample results from $\beta = 40\,\mathrm{K\,min^{-1}}$ compared to $10\,\mathrm{K\,min^{-1}}$

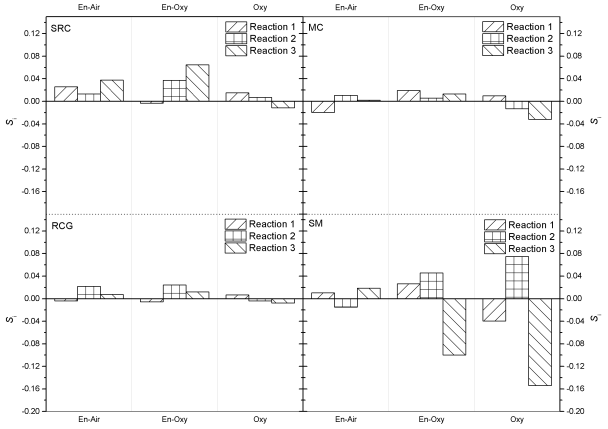

(a) $\beta = 10\,\mathrm{K\,min^{-1}}$

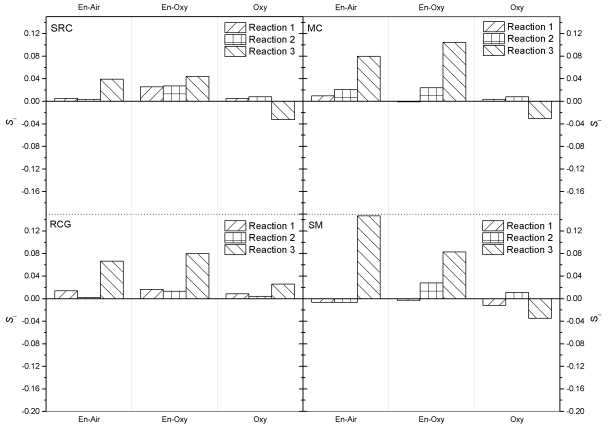

(b) $\beta = 40\,\mathrm{K\,min^{-1}}$

Figure 5: Changes in reactivity and temperature of maximum rate for short rotation coppiced (SRC) willow, miscanthus (MC) reed canary grass (RCG) and shea meal (SM) decomposing in different combustion atmospheres at a heating rates (β) of 10 and 40 $40\,\mathrm{K\,min^{-1}}$

Table .3: Results for fuel decompositions in various combustion atmospheres

Identifier (Atmosphere_β)	Rxn # (θ)	Temperature Range (K) Reaction	Leading Edge	Mass Fraction	CR Fit r^2	E_A kJ mol^{-1}	ln A	Reconstruct (r^2) Mass	DTG
SRC									
Air_10	1	488-572	524-554	0.24	0.9992	114.74	19.85		
	2	572-662	594-606	0.51	0.9994	188.25	32.48	0.9978	0.8194
	3	662-759	716-732	0.24	0.9944	173.66	23.82		
Air_40	1	510-594	546-576	0.23	0.9993	118.67	21.12		
	2	594-688	615-632	0.50	0.9998	175.10	29.74	0.9984	0.8698
	3	687-808	755-774	0.27	0.9967	143.75	18.68		
En-Air_10	1	496-570	530-552	0.24	0.9996	124.76	22.16		
	2	570-660	592-604	0.52	0.9992	196.67	34.39	0.9971	0.8055
	3	660-750	714-724	0.24	0.9959	196.92	28.07		
En-Air_40	1	514-594	548-576	0.24	0.9995	122.23	21.87		
	2	594-690	614-628	0.50	0.9999	177.50	30.26	0.9978	0.8515
	3	689-794	746-766	0.26	0.9937	162.03	21.92		
En-Oxy_10	1	494-574	524-552	0.27	0.9997	115.12	19.85		
	2	574-658	594-606	0.49	0.9998	230.74	41.36	0.9961	0.8221
	3	658-754	720-740	0.24	0.9945	229.00	33.60		
En-Oxy_40	1	513-590	551-576	0.23	0.9988	131.46	24.01		
	2	590-678	612-620	0.51	0.9999	194.40	33.95	0.9981	0.8410
	3	678-788	726-748	0.27	0.9955	154.14	20.96		
Oxy_10	1	494-572	526-556	0.24	0.9995	120.90	21.24		
	2	572-654	594-604	0.49	0.9995	193.74	33.67	0.9985	0.8293
	3	654-750	716-738	0.27	0.9877	164.79	22.35		
Oxy_40	1	516-595	551-572	0.24	0.9998	123.18	22.04		
	2	595-684	615-628	0.48	0.9999	183.28	31.38	0.9911	0.8920
	3	683-814	755-778	0.28	0.9978	130.15	16.38		
RCG									
Air_10	1	494-570	520-556	0.28	0.9999	132.09	23.82		
	2	570-640	590-606	0.45	1.0000	171.61	29.43	0.9990	0.9360
	3	640-768	672-710	0.27	0.9999	109.80	13.06		
Air_40	1	510-594	538-576	0.30	0.9999	132.12	24.07		
	2	594-666	607-626	0.41	0.9981	190.60	33.17	0.9989	0.9641
	3	666-826	700-754	0.29	0.9995	97.55	11.24		
En-Air_10	1	492-570	524-556	0.29	0.9997	129.82	23.32		
	2	570-636	586-598	0.44	0.9997	188.19	32.99	0.9989	0.9370
	3	636-762	670-710	0.28	0.9997	108.88	13.05		
En-Air_40	1	514-590	539-574	0.28	0.9999	139.59	25.80		
	2	590-664	606-620	0.44	0.9991	184.95	32.26	0.9989	0.9509
	3	664-806	703-742	0.28	0.9999	108.70	13.42		
En-Oxy_10	1	494-570	524-554	0.29	0.9998	128.84	23.11		
	2	570-636	586-598	0.44	0.9997	190.39	33.46	0.9988	0.9335
	3	636-760	668-712	0.27	0.9996	109.16	13.14		
En-Oxy_40	1	512-590	539-576	0.29	0.9998	140.93	26.11		
	2	590-664	606-618	0.43	0.9995	197.71	34.87	0.9986	0.9402
	3	664-800	700-740	0.28	0.9999	111.94	14.02		
Oxy_10	1	494-568	526-554	0.26	0.9998	133.48	24.23		
	2	568-640	588-600	0.46	1.0000	166.23	28.39	0.9990	0.9280
	3	640-768	678-716	0.28	0.9997	108.21	12.78		
Oxy_40	1	509-590	539-570	0.28	0.9998	134.61	24.74		
	2	590-664	605-620	0.43	0.9993	186.94	32.67	0.9989	0.9571
	3	664-824	700-746	0.29	0.9996	101.22	11.97		

Table .3: Results for fuel decompositions in various combustion atmospheres (cont.)

Identifier (Atmosphere_β)	Rxn # (θ)	Temperature Range (K) Reaction	Leading Edge	Mass Fraction	CR Fit r^2	E_A kJ mol^{-1}	ln A	Reconstruct (r^2) Mass	DTG
MC									
Air_10	1	500-578	528-562	0.31	0.9999	136.16	24.31		
	2	578-648	596-608	0.44	0.9999	216.26	38.25	0.9988	0.9482
	3	648-772	700-738	0.25	0.9953	121.07	14.72		
Air_40	1	520-600	554-587	0.30	0.9997	140.52	25.47		
	2	600-674	614-630	0.44	0.9989	199.77	34.69	0.9988	0.9691
	3	673-820	730-772	0.26	0.9986	104.61	12.18		
En-Air_10	1	498-578	526-568	0.30	0.9997	123.43	21.61		
	2	578-640	592-606	0.43	0.9999	228.21	40.80	0.9992	0.9408
	3	640-766	672-728	0.27	0.9986	116.52	14.19		
En-Air_40	1	524-600	560-588	0.31	0.9996	148.68	27.21		
	2	600-672	612-626	0.44	0.9983	230.95	40.96	0.9984	0.9636
	3	672-788	724-760	0.25	0.9973	122.32	15.48		
En-Oxy_10	1	502-572	530-560	0.28	0.9997	141.72	25.80		
	2	572-644	590-604	0.46	0.9998	210.10	37.37	0.9985	0.9223
	3	644-758	688-728	0.26	0.9970	120.77	14.87		
En-Oxy_40	1	519-600	552-584	0.31	0.9998	140.28	25.40		
	2	600-674	612-624	0.43	0.9982	236.86	42.15	0.9982	0.9562
	3	674-800	729-754	0.26	0.9978	133.41	17.35		
Oxy_10	1	500-574	528-560	0.28	0.9999	138.09	24.90		
	2	574-646	592-604	0.46	0.9999	194.64	33.98	0.9990	0.9307
	3	646-776	692-738	0.27	0.9964	113.70	13.39		
Oxy_40	1	525-602	552-578	0.31	0.9998	145.30	26.43		
	2	602-676	618-628	0.42	0.9995	215.78	37.77	0.9981	0.9593
	3	676-825	730-770	0.27	0.9991	100.20	11.33		
SM									
Air_10	1	455-534	494-524	0.12	0.9975	100.31	18.38		
	2	534-686	548-578	0.55	0.9911	116.18	18.25	0.9766	0.4936
	3	686-784	738-752	0.33	0.9914	208.79	28.47		
Air_40	1	461-554	504-540	0.14	0.9989	98.63	18.51		
	2	554-698	569-596	0.43	0.9932	119.43	19.56	0.9874	0.5912
	3	698-868	760-788	0.44	0.9984	97.52	10.18		
En-Air_10	1	445-532	504-518	0.12	0.9985	101.76	18.85		
	2	532-685	548-578	0.57	0.9936	111.44	17.25	0.9797	0.5298
	3	685-776	734-748	0.31	0.9925	218.14	30.31		
En-Air_40	1	460-554	500-540	0.14	0.9989	96.22	17.95		
	2	553-708	570-596	0.47	0.9936	117.95	19.19	0.9839	0.5829
	3	708-842	757-776	0.39	0.9988	138.10	16.90		
En-Oxy_10	1	472-536	494-518	0.13	0.9998	112.45	21.17		
	2	536-684	550-572	0.57	0.9935	131.65	21.67	0.9708	0.5002
	3	684-808	742-756	0.30	0.9938	152.17	18.86		
En-Oxy_40	1	460-554	498-540	0.14	0.9990	97.98	18.34		
	2	554-694	569-594	0.44	0.9936	130.38	21.97	0.9872	0.6559
	3	693-858	748-768	0.42	0.9941	110.97	12.64		
Oxy_10	1	454-538	486-524	0.14	0.9993	91.60	16.15		
	2	538-688	548-570	0.53	0.9881	147.06	24.97	0.9677	0.5134
	3	688-826	750-766	0.33	0.9956	139.24	16.45		
Oxy_40	1	460-556	502-540	0.14	0.9990	95.52	17.72		
	2	556-704	572-594	0.44	0.9941	125.92	20.86	0.9854	0.5861
	3	703-890	767-792	0.42	0.9988	94.31	9.52		